Wind-terrain effects on the propagation of wildfires in rugged terrain: fire channelling

Jason J. Sharples[1,2], Richard H.D. McRae[2,3], Rodney O.Weber[1,2] and Stephen R.Wilkes[1,4]

1. School of Physical, Environmental and Mathematical Sciences, University of New South Wales at the Australian Defence Force Academy. Canberra, ACT, Australia.
2. Bushfire Cooperative Research Centre. East Melbourne, Australia.
3. ACT Emergency Services Agency. ACT, Australia.
4. Fire Management Unit. ACT Parks, Conservation and Lands. ACT, Australia.

Corresponding author: Jason Sharples

j.sharples@adfa.edu.au

Suggested running head: Wind-terrain effects on wildfire propagation

Abstract

The interaction of wind, terrain and a fire burning in a landscape can produce a variety of unusual yet significant effects on fire propagation. One such example, in which a fire exhibits rapid spread in a direction transverse to the synoptic winds as well as in the usual downwind direction, is considered in this paper. This type of fire spread, which is referred to as 'fire channelling', is characterised by intense lateral and downwind spotting and production of extensive flaming zones. The dependence of fire channelling on wind and terrain is analysed using wind, terrain and multispectral fire data collected during the January 2003 alpine fires over southeastern Australia. As part of the analysis a simple terrain-filter model is utilised to confirm a quantitative link between instances of fire channelling and parts of the terrain that are sufficiently steep and lee-facing. By appealing to the theory of wind-terrain interaction and the available evidence, a number of processes that could produce the atypical fire spread are considered and some discounted. Based on the processes that could not be discounted, and a previous analysis of wind regimes in rugged terrain, a likely explanation for the fire channelling phenomenon is hypothesised. Implications of fire channelling for bushfire risk management are also discussed.

1. Introduction

The January 2003 alpine fires in southeastern Australia were notable in many ways. In particular, under extreme weather conditions on the afternoon of 18 January, fires originating to the west of Canberra (Fig. 1) impacted the national capital with tragic consequences (Nairn 2003). The Canberra fires also stand out as some of the best documented wildfires in Australia. The fires were documented in the form of airborne and land-based photographs and video, satellite data, and fire data that was recorded by a multispectral line-scanning instrument fitted to an aircraft that flew several missions over fire affected regions. These data sources permit analyses of the extreme fire behaviour experienced during the event. Moreover, as controlled experiments at the scale of the fire behaviour experienced on 18 January are not possible, these data sources provide rare opportunities to gain insight into the mechanisms driving the spread of large wildfires. Additional insight is obtained from similar material gathered after the fires, recording the severity of impact on the landscape. Analyses of data collected to the west of Canberra on the afternoon of 18 January have identified a number of processes associated with the extraordinary intensity of the fires (e.g. Dold et al. 2005; Fromm et al. 2006; Mills 2006; Mitchell et al. 2006). A review of the general meteorology surrounding the event is given by Taylor and Webb (2005).

The terrain to the west of Canberra is dominated by a sequence of rugged mountain ridges and valleys that are aligned roughly in a north-south direction with a maximum relief of about 1km. Given the complex terrain in which the fires burnt and the strong winds experienced during their most devastating runs towards Canberra, it is natural to consider the concept of wind-terrain interaction and to investigate what significance interaction between the wind and the terrain may have had on the development of the fires. Wind-terrain interaction, which refers to the way that the state of the fluid air (the wind) is affected by terrain features, can occur over a variety of spatiotemporal scales depending on the atmospheric structure, characteristics of the synoptic wind flow and the details of the topography (Wippermann and Gross 1981; Barry 1992; Whiteman and Doran 1993; Weber and Kauffmann 1998; Whiteman 2000). Understanding how local and regional winds can be modified through microscale and mesoscale wind-terrain interaction, and how modified winds might interact with a fire, are important problems when attempting to model the propagation of wildfires in complex terrain. Unexpected changes in wind direction and strength have been linked with several incidents where experienced fire fighters working in rugged terrain, have been killed or injured due to a sudden escalation in the severity of fire behaviour (Rothermel 1993; Butler et al. 1998; Cheney et al. 2001; Butler et al. 2003).

In this paper we identify and discuss a number of features in the multispectral line-scan data collected on the afternoon of 18 January that consistently suggest a link between atypical fire propagation and steep parts of the terrain that align with the prevailing winds in a certain way. These features are also complemented by a number of photographs and post-fire data. The atypical spread is characterised by rapid lateral propagation of the flank (often including lateral spotting) across a steep, lee-facing slope; distinctive darker smoke and vigorous plume behaviour of the advancing flank; downwind extension of the flaming zone of 2-5 km with uniform spectral signature in the imagery; and the upwind edge of the flaming zone constrained by a major break in topographic slope. We refer to instances of the atypical fire spread as 'fire channelling' events. By applying a simple terrain-filter model to the available data, a quantitative connection between certain regions of the landscape and instances of fire channelling is established. By appealing to the theory of meso- and micro-scale wind-terrain interactions, and a previous analysis of wind regimes in complex terrain (Sharples et al. 2010a), we propose a plausible mechanism that accounts for the atypical propagation.

2. Data and methods

2.1 Wind and terrain data

Wind data for 18 January 2003 were recorded at Canberra Airport and at the Emergency Services Bureau Headquarters at Curtin (see Fig. 1 for locations). Fig. 2 indicates that wind speeds averaged around 30-40 km h^{-1} during the most intense fire activity, reaching a maximum of just under 50 km h^{-1} at 15:30, while the wind direction contributing to the most devastating fire runs varied between west-northwest and northwest. The daily aerological sounding at Wagga Wagga (the closest sounding station to Canberra, approx. 160 km to the west) indicated that winds were from the west throughout the vertical extent of the atmosphere sampled, with the exception of the near surface winds that had a more northerly component.

Terrain data for the region of interest is derived from the 90m resolution Shuttle Radar Topography Mission data (Farr et al. 2007). This digital elevation model (DEM) was rescaled to 250m resolution and was used to derive gridded slope and aspect data within the GIS software MapInfo Professional™.

2.2 Multispectral line-scan data

A small aircraft carrying a Daedalus 1268 airborne thematic mapper (ATM) instrument was tasked to fly parallel traverses of the fire complex on 18 January. The

Daedalus 1268 ATM, sometimes referred to as a multispectral line-scanning instrument, collects radiance measurements in twelve spectral bands covering the visible and infrared spectrum (Harrison & Jupp 1989). Data is collected as digital numbers representing radiance on a scale of 0 to 255, in multiple lines as the sensor sweeps back and forth. Inertial navigation data is stored in an additional band to allow orthorectification of the data with respect to the underlying topography (Cook et al. 2009). The regions covered by the respective scan runs can be seen in Fig. 3.

Interpretation of multispectral line-scan data of dynamic events such as bushfires can disclose a significant amount of information. To aid in their interpretation, processing of the line-scan data is conducted to create a standard operational image for bushfire managers. The processing is intended to give key features a consistent pseudo-colour, and is based on the assignment of three spectral bands as coordinates in the three dimensional red-green-blue (RGB) colour system (Cook et al. 2009). Specifically, the assignment is given in Table 1 along with some indicative RGB coordinate values for image features. The use of pseudo-colouring aids in image interpretation by providing enhanced discrimination of the features captured in the imagery, beyond that which is possible using a single spectral band (Cook et al. 2009). The contents of Table 1 were derived through analyses of the line-scan imagery by the authors, in conjunction with extensive consultation with remote sensing experts (R. Cook, A. Walker, R. Norman, pers. comm.). We stress that the coordinate values listed in Table 1 are indicative only – while appropriate image processing will remove nearly all of the cloud and smoke from the images, the presence of heavy smoke will cause some variability about the RGB coordinate values listed in Table 1, as will the characteristics of the surface, especially when the edge of the scan coincides with sharp terrain features. Examples of these effects can be seen in the southeast corner of Fig. 5b just below point 2. In this case the signal from within the incised valley that runs through the centre of the figure (Flea Creek) is being affected by both heavy smoke (evident in Fig. 5c) and is being partially blocked by the large ridge immediately upwind of the Flea Creek valley.

Examination of the line-scan data collected on 18 January revealed a number of interesting events. The general locations of five of these events are indicated in Figs. 1b and 1c. We note that three events occurred in close proximity at the location labelled 'Broken Cart event' in Fig. 1c. The following subsections provide more detail on four of these five events.

2.2.1 Bendora Dam

Fig. 4 shows line-scan imagery of the Bendora Dam fire after it flared up at approximately 14:30 on 18 January (Cheney 2003). The location of the flare up can be seen as a small orange area, circled in Fig. 4a. Fig. 4a indicates that at 14:46 the fire had developed laterally as well as downwind resulting in a large expanse of active flame (Table 1). The direction of lateral spread is almost due south, approximately perpendicular to the synoptic wind direction. Fig. 4a also indicates that active flaming at the flare up location was only just starting to decay (as indicated by the darker orange colour) by the time the fire had spread laterally to point 1. This means that the fire had spread a distance of approximately 2 km within the burn-out time for flaming combustion. Indeed, if the flare up occurred at approximately 14:30, Fig. 4a indicates a lateral rate of spread of around 7.5 km h^{-1}. Fig 4a also indicates that spot fires were forming across the flank: for example, a spot of active flame can be seen to the south of the flank just above point 2.

Fig. 4b shows the same area 46 minutes later and indicates that the fire continued its lateral propagation. The overlapping line-scan images (Figs. 4a and 4b) suggest that the fire spread at least 2.7 km from point 1 to point 3, implying a lateral rate of spread of at least 3.6 km h^{-1}. Note that according to the McArthur mark 5 Forest Fire Danger Meter (McArthur 1967; Noble et al. 1980), under extreme fire danger conditions (FFDI = 100) and assuming a fuel load of 25 t ha^{-1}, the head-fire rate of spread (in the direction of the wind) is only expected to be 3 km h^{-1} (in the absence of a topographic gradient).

The upwind edge of the flaming zone in Figs. 4a and 4b is constrained by the rim of the lower incised valley. The dark smoke and strong convection visible near point 4 on the southern flank in Fig. 4c indicates rapid and intense combustion on the advancing flank.

2.2.2 McIntyre-Goodradigbee

Fig. 5 shows the development of the of the McIntyre's Hut fire between 14:30 and 15:00 on 18 January. Of particular interest is the development of the south-western part of the fire after a spill-over occurred near the location circled in Figs. 5a and 5b. Fig. 5b indicates that this part of the fire spread laterally along the Goodradigbee River valley. Fig. 6 shows line-scan imagery of the fire development at 15:13 and 15:22. Figs. 6a and 6b show that the fire has spread approximately 2km southwards along the incised valley, ultimately reaching point 1 where the fuel downwind of the fire was unburnt. Beyond this point the fire has escalated rapidly, spreading into and across the Flea Creek valley (point 3 in Fig. 6b). Photographs of the convection column (Fig. 7) and radar data suggest that this was the most intense fire event of the day (Fromm et al. 2006) and provide a direct link between the lateral spread and pyro-cumulonimbus (pyro-Cb) development.

Assuming that the spill-over occurred at approximately 14:30 (Cheney 2003), Fig. 6a indicates that the fire spread approximately 6 km to point 2, in a direction near perpendicular to the synoptic wind, in approximately 45 minutes. This amounts to a lateral rate of spread of about 8 km h^{-1}; a similar speed to that inferred in the Bendora Dam case. The lateral depth of active flame also attests to a very rapid rate of lateral spread. The dark smoke and vigorous convection evident near point 4 in Fig. 6c again indicates intense and rapid combustion on the advancing flank.

2.2.3 Broken Cart

The line-scan images of the fire development at Broken Cart (Fig. 8) indicate atypical lateral spread on both the northern and southern flanks. Specifically, the northern edge of the fire perimeter to the southwest of point 2 in Fig. 8b displays a distinct kink where the fire has propagated in a north-northeasterly direction with an extended region of active flame downwind. Several spot fires can be seen burning to the north of this flaming zone (just under point 2 in Fig. 8b), despite the fact that the synoptic winds were from the west-northwest. A similar right-angled kink on the southern flank, indicating fire spread towards the southwest, can be seen above point 1 in Fig. 8a, with an extended region of active flame again present downwind. Lateral spot fire development is also evident on this part of the fire, with successive spot fires visible as yellow spots of active flame near point 1 and point 3 in Fig. 8a and 8b, respectively. The upwind edges of the flaming zones on the northern and southern flanks both coincide with significant ridge lines of approximately 200-250m relief. This coincidence is most clearly seen near points 5 and 6 in Fig. 8c. Note that errors in the orthorectification process have resulted in a poor match between the fire edge and ridge line (as indicated by the contours) near point 3 in Fig. 8b. These errors are smaller in Fig. 8a and are not present at all in the visual band image shown in Fig. 8c.

While it is not possible to get absolute estimates of the lateral rates of spread in these cases, there is sufficient evidence to conclude that the lateral rate of spread was more rapid than that for typical flank fire spread by comparing the lateral depth of the flaming zones at different parts of the fire edge. For example, above point 4 in Fig. 8b, the line of (yellow) active flame has a lateral depth of 50m or less, while the lateral depth of active flame above point 3 is approximately 800m. Thus, assuming that the flaming combustion burn-out time is similar for the two forested regions near points 3 and 4, we may conclude that the lateral rate of spread near point 3 was significantly faster compared to the lateral spread near point 4. A similar argument can be invoked for the lateral spread near point 2 in Fig. 8b, where the lateral depth of active flame is approximately 400m. Moreover, the pattern and colour of smoke emanating from near points 5 and 6 in Fig. 8c again indicates that the most intense and rapid combustion occurred in association with the regions of lateral spread.

Note that the line-scan data in Fig. 8 only contains two of three events at Broken Cart. The third event, which developed after 15:09 near point 7 in Fig. 8c, was inferred from the shape of the fire perimeter in post-fire line-scan data and photographic evidence.

2.2.4 Common features

In the fire channelling cases just considered, a number of common features are evident. In particular, each case was characterised by:

- Rapid lateral propagation of the flank (i.e. in a direction transverse to the synoptic wind) along a valley or lee slope, including instances of lateral spot fire development
- Downwind extension of the flaming zone with uniform spectral signature for 2-5 km
- The upwind edge of the flaming zone constrained by a major break in topographic slope

Based on these defining characteristics it was possible to identify a number of additional instances of fire channelling. In total, twenty-three events were identified through similar diagnoses: fourteen on 18 January 2003 and an additional nine on 26 January 2003, in connection with fires that burnt in rugged terrain near the NSW-Victorian border.

3. Analysis of wind and terrain dependence

The fact that the lateral spread was constrained on its upwind edge by a major break in topographic slope suggests that the interaction of the strong synoptic winds with the rugged terrain plays an important role in driving the fire channelling phenomenon. To further investigate the role played by wind-terrain interaction, a simple terrain-filter model was developed for use as a diagnostic tool. The model is based on wind direction and topographic slope and aspect and is intended to distinguish those parts of the landscape where fire channelling was observed to have occurred.

The terrain-filter model takes the form of a characteristic function as follows:

$$\chi(\sigma,\delta) = \begin{cases} 1 & \text{if } \gamma_s \geq \sigma \text{ and } |\theta_w - \gamma_a| \leq \delta, \\ 0 & \text{otherwise.} \end{cases} \tag{1}$$

Here γ_s is the topographic slope angle, γ_a is the topographic aspect and θ_w is the direction that the synoptic wind is blowing towards (i.e. the standard wind direction ± 180°). The model is defined by the parameters σ and δ, which denote a threshold topographic slope angle and a threshold difference between the wind direction and topographic aspect, respectively. In plain terms, the model identifies parts of the landscape steeper than σ and with a topographic aspect within δ of the direction the synoptic winds are heading. For convenience we will refer to σ and δ as the 'slope threshold' and 'aspect discrepancy', respectively.

Using a geographic information system (MapInfo™) equation (1) was applied over the digital elevation model. The resulting grid (of 0's and 1's) was then compared to fire perimeter data derived from the line-scan imagery. By varying the parameters σ and δ in the model we sought to produce a grid that identified those parts of the landscape where fire channelling occurred. The model was thus calibrated by varying the parameters until the smallest subset of the landscape that contained the five locations identified in the events described in sections 2.2.1-2.2.3 was obtained.

Assuming a west-northwesterly synoptic wind direction of 305° (θ_w = 125°) over the regions of interest the calibrated model parameter values were found to be σ = 10.5°

and δ = 40°. Hence the calibrated model identifies parts of the landscape with topographic aspects between 85° and 165° and with topographic slopes above 10.5°. Note that the derived slope threshold value σ = 10.5° relates to a DEM of 250m resolution. To convert this to a value of topographic slope as would be perceived by a person actually within the landscape, we use the scaling formula of McRae (1997). Thus, assuming that slope is perceived at a scale of around 10-20 m, we obtain a value for the threshold slope of approximately 26-30°.

The calibrated model was then applied to the surrounding landscape, including those parts where other fire channelling events were observed. Fig. 9 shows how the output of the calibrated terrain-filter model compares with other locations where fire channelling was observed on 18 January. As can be seen in Fig. 9, each of the locations where the unusual fire spread occurred (thick black curves in Fig. 9) coincide with parts of the landscape identified by the terrain-filter model. The one exception is the 'Hyles Block South' event (top right of Fig. 9) for which the surrounding terrain was not properly resolved by the DEM used. Field reconnaissance of the region, however, confirmed a slope and aspect within the ranges stipulated by the terrain-filter model. In fact all twenty-three confirmed cases of fire channelling (including the five events used in the calibration) were successfully identified in such a way with the diagnostic model.

It is important to note that the fires passed over some of the regions identified by the terrain-filter model without displaying any atypical fire spread. This means that the model identifies a condition of the landscape that is necessary for occurrence of the atypical fire spread, but that is not sufficient in general. The complete set of conditions necessary for fire channelling to occur would also likely include non-topographic factors such as fuel structure, load and moisture content as well as synoptic wind speed and within-stand (microscale) atmospheric dynamics, including vertical airflow. Note also, however, that unusual fire spread similar to the events discussed may have occurred at some of the other regions identified by the model, but were not recorded in the line-scan imagery or formally recognised as an event of interest.

The wind-terrain analyses, implemented using the diagnostic model, therefore quantitatively confirm a spatial correspondence between fire channelling incidence and parts of the landscape that are sufficiently steep and lee-facing. The fact that all of the fire channelling events considered could be successfully classified in terms of topographic slope, topographic aspect and wind direction, is a strong indication that the atypical spread is due to an interaction between the wind and the terrain.

In fact, the terrain features identified by the model possess very similar characteristics to those identified by Sharples et al. (2010a) as having a very high likelihood of wind reversal when winds are strong. Indeed, Fig. 10 shows how the empirically derived probabilities of a wind reversal on various lee-slopes vary with synoptic wind speed, and indicates that when winds are over about 20-25 km h^{-1} and blowing from an approximately westerly direction, there is a greater than 90% chance that the wind will be blowing in a roughly opposite direction on a lee-slope. The process most likely to result in such a wind reversal is a lee-slope (separation) eddy (Wood 1995; 2000; Sharples et al. 2010a). Thus combining the results of Sharples et al (2010) with the results of the terrain-filter diagnoses, there is a high likelihood that when synoptic winds are strong, the steep, lee-facing parts of the terrain associated with fire channelling occurrence have a flow regime dominated by lee-slope eddies. These results give important guidance towards diagnosing the mechanism driving the fire channelling process.

4. Hypothetical mechanisms for the atypical spread

In this section we propose a number of processes that could account for the fire channelling phenomenon. In doing so we are lead to consider processes that can result in airflows that move in a direction transverse to the synoptic winds, and as such are able to support the lateral advection of fire and embers evident in the line-scan data. Using the available data in conjunction with the results of the analyses discussed in section 3 it is possible to discount a number of the hypothetical mechanisms.

4.1 Thermally-induced winds

Differences in insolation across complex topography can produce thermally-induced pressure gradients that cause winds to flow along slopes or incised valleys (Whiteman 2000; Sharples 2009). However, thermally-induced winds can be easily discounted as a driver of the atypical spread since any thermal effects would have been dominated by the strong synoptic winds experienced during the events considered (e.g. 30-45 km h^{-1}, gusting to 60-75 km h^{-1} during the 18 January events).

4.2 Pressure-driven channelling

Pressure-driven channelling (Fiedler 1983) occurs when the air within a valley responds to the component of the geostrophic pressure gradient along the valley axis (Wippermann and Gross 1981; Wippermann 1984; Gross and Wippermann 1987;

Kossmann and Sturman 2003; Sharples 2009, Fig. 3). However, since the direction of pressure-driven channelling is dictated by the alignment of the geostrophic pressure gradient with respect to the valley axis, if pressure-driven channelling was driving the lateral fire spread then it should occur in a single direction only. This is at odds with the line-scan data which shows lateral spread in both northerly and southerly directions. Moreover, the scale of the valleys in which the atypical spread was observed are too fine-scale to support pressure-driven channelling (Wippermann and Gross 1981; Whiteman and Doran 1993).

4.3 Forced channelling

Forced channelling results when the side-walls of a valley cause frictional differences that are much less in the along-valley direction than they are in the across-valley direction (Doran and Whiteman 1992; Whiteman and Doran 1993; Kossmann et al. 2001; Kossmann and Sturman 2002). These frictional differences force the wind to align preferentially along the valley axis, with the direction and strength of the channelled flow dependent upon the sign and magnitude of the component of the synoptic winds relative to the valley axis (Sharples 2009; Fig. 2;) and the details of the terrain (Kossmann and Sturman 2002).

It is not possible to completely rule out forced channelling as a driving mechanism. It is quite plausible that strong synoptic winds could be channelled along incised valleys that run almost perpendicular to the synoptic wind direction. However, forced channelling should occur whenever the surrounding topography favours it; particularly when winds encounter significant windward-facing slopes that act to divert it in a direction different to the synoptic winds. Thus if forced channelling is driving the atypical fire spread there doesn't seem to be any *prima facie* reason why steep, lee-facing slopes should be identified.

4.4 Downward momentum transport

Vertical mixing within the atmosphere can occur through a number of processes such as convective mixing (e.g. driven by a large fire) and gravity waves. Through this vertical mixing it is possible for upper winds to influence surface conditions. Conservation of momentum then dictates that when these upper winds are mixed down towards the surface, the surface winds will inherit some of the upper wind direction. For vertical wind profiles exhibiting directional shear, the downward transport of momentum can thus result in surface winds moving in a direction quite different to the synoptic wind.

However, if downward transport of momentum was driving the lateral spread then the spread should have only occurred in the one direction. As mentioned in subsection 4.x, this is contrary to what was documented. Furthermore, if momentum exchange with the upper levels of the atmosphere was driving the lateral spread then it would be expected to occur whenever and wherever the fire is able to produce sufficient vertical mixing. This is difficult to reconcile with the fact that the lateral spread only occurred in connection with steep, lee-facing slopes. Finally, we note that the atmospheric sounding at Wagga Wagga indicated that there was no directional shear in the profile.

4.5 Wind-terrain-fire interactions

When the synoptic winds are strong, airflows resembling forced channelling can also occur along the lee-slopes of mountain ranges, even without the presence of a definite valley. Under such circumstances a lee-rotor, or separation eddy, can form depending upon the steepness and roughness of the terrain, the speed of the synoptic winds and the stability of the atmosphere (Lee et al. 1981; Byron-Scott 1990; Papadopoulos et al. 1992; Wood 1995; 2000; Bowen 2003; Lewis et al. 2008; Sharples et al. 2010a). For example, Wood (1995) reports that for a neutral, turbulent flow, separation will generally occur when the lee-slope exceeds a critical inclination of approximately 20°.

The partial decoupling of the near-surface winds and the upper winds in the lee of a ridge also permits the generation of local winds that can flow with an across-slope component along the lee-slope with a speed and direction dictated by the across-slope component of the synoptic winds, local pressure gradients or thermal influences. For example, if the synoptic winds are not quite perpendicular to a ridge, the airflow near the surface in its lee can inherit an across-slope component through conservation of momentum. Alternately, it is possible that the flow within the separation eddy could acquire an across-slope component due to thermal effects or the emergence of local pressure gradients (such as those that would result from the presence of a fire). The net effect in all of these cases is for the air to follow a helical pattern about a horizontal axis aligned approximately parallel to the ridgeline. This phenomenon has been termed lee-slope channelling by McRae (2004), who first postulated its role during the 2003 Canberra fires.

The analyses of wind and terrain dependence coupled with the probabilistic analyses of Sharples et al. (2010a) provides a strong indication that a lee-slope eddy plays a key role in driving the fire channelling process. Moreover, if a fire happened to spread into a region affected by a separation eddy, then the hot gas from the fire could be entrained within the eddy, with the strong wind shear at the top of the eddy impeding mixing between the synoptic and separated flows. Hence, supposing a fire enters a region of separated flow at the north end of a slope or valley, and treating the air within the eddy as a quasi-isolated system (i.e. a system that involves only limited mixing with the surrounding environment), cf. Byron-Scott (1990), the air within the northern part of the eddy will be at a higher temperature and pressure than the air within the southern part of the eddy. As a consequence the air within the eddy will tend to move towards the south in response to the thermally-induced pressure gradient or simply due to thermal expansion of the air within the eddy. Based on the available evidence such an interaction constitutes the most likely mechanism driving the atypical spread.

Wind-terrain-fire interactions like that just discussed also account for some of the other observed fire channelling characteristics. Once a bushfire enters a region prone to eddy formation, the fire can act to intensify the vortical flow through buoyant enhancement (Byron-Scott 1990) and the increased turbulence can facilitate more efficient production of embers, which are then circulated with the eddy. Then, in addition to being transported laterally within the eddy in response to the fire-induced thermal/pressure gradient, a proportion of the embers can be ‘peeled off’ from the top of the eddy by the synoptic winds and deposited downwind where they ignite further spot fires that grow and amalgamate. The bidirectional nature of the process, with embers advected both laterally within the separated flow and downwind by the synoptic flow, means that it can rapidly and efficiently spread a fire across a landscape. The result of the process is an extensive region of active flame, not unlike those observed in the line-scan imagery.

Fig. 11 provides a schematic view of the wind-terrain-fire interaction described above.

4.6 Other factors

A number of other factors could potentially account for the atypical spread. These include changes in wind direction over time, spatial changes in fuels and fire control operations. However, for the fire channelling events on 18 January it is known that these factors did not influence the fire propagation. An additional mechanism that could account for lateral spread is plume interaction. When two large fire plumes form in sufficiently close proximity, the associated indraft can cause the respective fires to draw towards each other, possibly in a direction that differs significantly to the synoptic wind direction. This mechanism could possibly account for the lateral spread of the Bendora fire which was in reasonably close proximity to the Stockyard Spur fire (visible to the SW in Fig. 4a) and a more northerly breakout of the (old) Bendora fire (visible to the NE in Fig. 4a). However, in this case the authors are unaware of any evidence that supports the presence of a significant indraft. Moreover, if plume interaction had driven the lateral spread, the expectation would have been for the Bendora fire to spread laterally to the north, towards the closer and more energetic plume emanating from the northerly Bendora breakout, rather than to the south. Finally, lateral spread driven by plume interaction is difficult to reconcile with the fact that the lateral spread was constrained by the windward ridge of a steep, lee-slope.

5. Discussion and conclusions

A number of instances of atypical fire propagation have been presented and discussed. These instances involved rapid, bidirectional fire spread transverse to, as well as in the direction of the synoptic winds, the lateral development of spot fires and the formation of extensive regions of active flaming. We refer to these instances as 'fire channelling'. Examination of the characteristics of fire channelling events and consideration of empirical wind direction data collected over nearby rugged terrain suggested that the process was most likely due to the interaction of a bushfire with a lee-slope eddy. Indeed, steep slopes over about 25° and topographic aspects within about 30° of the direction the wind is blowing were found to be necessary conditions for the occurrence of the fire channelling phenomenon. Other factors that are also likely to be important in determining whether the fire channelling process will occur include wind speed, fuel moisture, fuel structure, spatial distribution of vegetation and atmospheric stability.

To gain a better understanding of the process it is important to continue recording the evolution of large fires using line-scan and other airborne technology and to supplement these data, where possible, with detailed meteorological measurements. As additional cases of fire channelling are confirmed through analyses of data (e.g. line-scan imagery) they provide further opportunities to develop tools to predict their occurrence. Further refinement of the terrain-filter diagnostic is one possible approach. Small-scale combustion tunnel experiments and development of appropriate physical (numerical) models could also be used to evaluate the conclusions drawn above and will be the subject of further work by the authors. In fact, in this respect it is worth noting the results of recent combustion tunnel experiments conducted by Sharples et al. (2010b), which tend to support the above conclusions.

The fire channelling phenomenon has clear implications for fire management and for fire fighter safety. Fire channelling is a very efficient mechanism for spreading a fire across a landscape, and the intense and expansive fire behaviour associated with it increases the likelihood of a fire transitioning to the plume-driven phase (Chatto 1999). This is clear in the case of the McIntyre's Hut fire, for example. Furthermore, the rapid escalation of a small fire due to fire channelling can result in a catastrophic decay in both fire-fighter and community safety that is counter-intuitive. In this paper we have established the existence of fire channelling, detailed its distinguishing characteristics, and proposed a hypothetical mechanism to explain its occurrence. These constitute the first steps in deducing effective measures to manage the incidence and effects of fire channelling at a time when wildfires are an increasing global environmental problem.

Acknowledgements

The authors are grateful to Assoc. Prof. R.O. Weber for advice and discussion on the topic of the paper. J.J. Sharples would also like to thank Dr. A.M. Gill for helpful discussion and advice. This work was undertaken as part of the Bushfire CRC's HighFire Risk project. The support of the Bushfire CRC is acknowledged. The authors are also indebted to the anonymous reviewers whose comments contributed to improvements in the original version of the manuscript.

References

Barry RG (1992) *Mountain weather and climate*. 2nd edition. Routledge, New York.

Bowen AJ (2003) Modelling of strong wind flows over complex terrain at small geometric scales. *Journal of Wind Engineering and Industrial Aerodynamics*, **91**, 1859-1871.

Butler BW, Bartlette RA, Bradshaw LS, Cohen JD, Andrews PL, Putnam T, Mangan RJ, Brown H (1998) Fire Behavior Associated with the 1994 South Canyon Fire on Storm King Mountain, Colorado. US Forest Service Research Paper RMRMS-RP-9.

Butler BW, Bartlette RA, Bradshaw LS, Cohen JD, Andrews PL, Putnam T, Mangan RJ, Brown H (2003) The South Canyon Fire Revisited: Lessons in Fire Behaviour. *Fire Management Today* **63**(4), 77-84.

Byron-Scott RAD (1990) The effects of ridge-top and lee-slope fires upon rotor motions in the lee of a steep ridge. *Mathematical and Computer Modelling*, **13**(12), 103-112.

Cook R, Walker A, Wilkes S (2009) Airborne fire intelligence. In: *Innovations in remote sensing and photogrammetry*. (Eds S Jones, K. Reinke) pp. 239-254 (Springer: Heidelberg)

Chatto K (Ed.) (1999) Development, behaviour, threat and meteorological aspects of a plume-driven bushfire in west-central Victoria: Berringa Fire February 25-26, 1995. Research Report No. 48. Fire Management, Department of Natural Resources and Environment.

Cheney P, Gould JS, McCaw L (2001) The dead-man zone: a neglected area of fire fighter safety. *Australian Forestry*, **64**, 45-50.

Cheney, N.P. (2003) *The January 2003 ACT fires – report for the ACT Coroner*. Powerpoint Presentation. (Available from ACT Coroner's Court upon request).

Dold J, Weber RO, Gill AM, Ellis P, McRae R, Cooper N (2005) Unusual Phenomena in an Extreme Bushfire. In: *Proceedings of the 5th Asia-Pacific Conference on Combustion*, 17-20 July 2005, The University Adelaide, South Australia.

Doran JC, Whiteman CD (1992) The coupling of synoptic and valley winds in the Tennessee valley. In: *Proceedings of the 6th conference on mountain meteorology*. American Meteorological Society, Boston.

Farr TG, Rosen PA, Caro E, Crippen R, Duren R, Hensley S, Kobrick M, Paller M, Rodriguez E, Roth L, Seal D, Shaffer S, Shimada J, Umland J, Werner M, Burbank D, Alsdorf D (2007) The Shuttle Radar Topography Mission. *Reviews of Geophysics*, 45, RG2004, doi: 10.1029/2005RG000183.

Fiedler F (1983) Einige characteristika der strömungen im oberrheingraben. *Wissenschaftliche Berichte des Meteorologischen Instituts der Universität Karlsruhe*, **4**, 113-123.

Fromm M, Tupper A, Rosenfeld D, Servranckx R, McRae R (2006) Violent pyro-convective storm devastates Australia's capital and pollutes the stratosphere, *Geophysical Research Letters*, **33**, L05815

Gross G, Wippermann F (1987) Channelling and countercurrent in the upper Rhine valley: numerical simulations. *Journal of Climate and Applied Meteorology*, **26**, 1293-1304.

Harrison BA, Jupp DLB (1989) *Introduction to remotely sensed data*. CSIRO Australia.

Kossmann R, Sturman A, Zawar-Reza P (2001) Atmospheric influences on bush fire propagation and smoke dispersion over complex terrain. In: *Proceedings, 2001 Australasian Bushfire Conference*, Christchurch NZ.

Kossman M, Sturman AP (2002) Dynamic airflow channelling effects in bent valleys. In: *Proceedings of the 10th conference on mountain meteorology.* 17-21 June 2002, Park City UT. American Meteorological Society.

Kossman M, Sturman AP (2003) Pressure-driven channelling effects in bent valleys. *Journal of Applied Meteorology*, **42**(1), 151-158.

Lee JT, Barr S, Snyder WH, Lawson RE Jnr (1981) Wind tunnel studies of flow channelling in valleys. In: *Proceedings of the 2nd conference on mountain meteorology.* 9-12 November 1981. Steamboat Springs CO. American Meteorological Society.

Lewis HW, Mobbs SD, Lehning M (2008) Observations of cross-ridge flows across steep terrain. *Quarterly Journal of the Royal Meteorological Society*, **134**, 801-816.

McArthur AG (1967) Fire behaviour in eucalypt forests. Department of National Development, Forestry and Timber Bureau Leaflet No. 107. Canberra, Australia.

McRae RHD (1997) Considerations on operational wildfire spread modelling. In: *Proceedings, Bushfire 1997. Australian Bushfire Conference*, July 1997, Darwin.************** Available from website*************

McRae RHD (2004) Breath of the dragon – observations of the January 2003 ACT Bushfires. In: *Proceedings of 2004 Australasian Bushfire Research Conference*, May 2004, Adelaide.

Mills GA (2006) On the sub-synoptic scale meteorology of two extreme fire weather days during the Eastern Australian fires of January 2003. *Australian Meteorological Magazine*, **54**, 265-290.

Mills GA (2007) On easterly changes over elevated terrain in Australia's southeast. *Australian Meteorological Magazine*, **56**, 177-190.

Mitchell RM, O'Brien DM, Campbell SK (2006) Characteristics and radiative impact of the aerosol generated by the Canberra firestorm of January 2003. *Journal of Geophysical Research*, **111**, D02204

Nairn G (Chair) (2003) *A Nation Charred: Inquiry into the Recent Australian Bushfires*. The Parliament of the Commonwealth of Australia, Canberra.

Noble IR, Bary GAV, Gill AM (1980) McArthur's fire-danger meters expressed as equations. *Australian Journal of Ecology*, **5**, 201-203.

Papadopoulos KH, Helmis CG, Amanatidis GT (1992) An analysis of wind direction and horizontal wind component fluctuations over complex terrain. *Journal of Applied Meteorology,* **31**, 1033-1040.

Rothermel RC (1993) Mann Gulch Fire: A Race That Couldn't Be Won. US Forest Service General Technical Report INT-299. May 1993.

Sharples JJ (2009) An overview of mountain meteorological effects relevant to fire behaviour and bushfire risk. *International Journal of Wildland Fire*, **18**, 737-754.

Sharples JJ, McRae RHD, Weber RO (2010a) Wind characteristics over complex terrain with implications for bushfire risk management. *Environmental Modelling and Software*, **25**, 1099-1120.

Sharples JJ**,** Viegas DX, Rossa CG, McRae RHD (2010b) Small-scale observations of atypical fire spread caused by the interaction of wind, terrain and fire. In: DX

Viegas (ed.) *Proceedings of the VI International Conference on Forest Fire Research*, November 2010, Coimbra, Portugal.

Taylor J, Webb R (2005) Meteorological aspects of the January 2003 south-eastern Australian bushfire outbreak. *Australian Forestry*, **68**(2), 94-103.

Webb R, Davis C, Lleyett S (2004) Meteorological aspects of the ACT bushfires of January 2003. Proceedings of the Conference *Bushfire 2004: Earth, Wind and Fire - Fusing the Elements.* South Australian Department of Environment and Heritage, Adelaide, South Australia.

Weber RO, Kauffmann P (1998) Relationship of synoptic winds and complex terrain flows during the MISTRAL field experiment. *Journal of Applied Meteorology*, **37**, 1486-1496.

Whiteman CD, Doran JC (1993) The relationship between overlying synoptic-scale flows and winds within a valley. *Journal of Applied Meteorology*, **32**, 1669-1682.

Wippermann F (1984) Air flow over and in broad valleys: channelling and counter-current. *Contributions to Atmospheric Physics*, **57**, 92-105.

Wippermann F, Gross G (1981) On the constriction of orographically influenced wind roses for given distributions of the large-scale wind. *Beitraege zur Physik der Atmosphere*, **54**, 492-501.

Whiteman CD (2000) *Mountain Meteorology: Fundamentals and Applications*. Oxford University Press.

Wood N (1995) The onset of separation in neutral, turbulent flow over hills. *Boundary-Layer Meteorology*, **76**, 137-164.

Wood N (2000) Wind flow over complex terrain: a historical perspective and the prospect for large-eddy modelling. *Boundary-Layer Meteorology*, **96**, 11-32.

Table and Figure Captions

Table 1. Indicative Red-Green-Blue coordinate values for features in images with well balanced pixel intensity distribution.

Figure 1. Wind speed (grey lines), gust (black lines) and direction (boxes) data recorded at (a) Canberra Airport and (b) Curtin Emergency Services Bureau Headquarters on 18 January 2003.

Figure 2. Aerological diagram derived from rawinsonde ascent at Wagga Wagga, 00:00 UTC 18 January 2003.

Figure 3. (a) Map of southeastern Australia showing the locations of events considered in the study, (b) Map showing the locations of the Flea Creek, Broken Cart and Bendora Dam events in relation to the main geographic features and topography of the region.

Figure 4. Multispectral line-scan data for the Bendora Dam Fire overlayed on DEM data (100 m contours). (a) Bendora Dam event imaged at 14:46 [Run 2], (b) Bendora Dam event imaged at 15:32 [Run 6], clearly moving southwards, (c) Visual band image of Bendora Dam event at 14:46 [Run 2]. The circled region in (a) is where the fire reignited. The arrow in (a) indicates the synoptic wind direction, while the grey line indicates the approximate location of the fire perimeter prior to 18 January 2003. The horizontal lines evident in panel (b) are a consequence of the turbulent

environment in which the aircraft carrying the line-scanning instrument was operating.

Figure 5. Multispectral line-scan data for the McIntyre's Hut Fire overlayed on DEM data (100 m contours). (a) Flea Creek – Goodradigbee River part of the McIntyre's Hut Fire imaged at 15:13 [Run 4], (b) Flea Creek – Goodradigbee River part of the McIntyre's Hut Fire imaged at 15:22 [Run 5], (c) Visual band image of the Flea Creek – Goodradigbee River part of the McIntyre's Hut Fire imaged at 15:22 [Run 5]. The arrow in (a) indicates the synoptic wind direction, while the grey line indicates the approximate location of the fire perimeter prior to 18 January 2003. The region circled in black marks the approximate position where the fire flared up.

Figure 6. (a) Photograph of the fire channelling events at Flea Creek (McIntyre's Hut fire) and Brindabella Rd Lower (Photo taken by local resident), (b) Photograph of a well developed pyro-Cb over the McIntyre's Hut fire 24 minutes after the line-scan imagery in Fig. 4b was recorded (Photo taken by S.R. Wilkes)

Figure 7. Multispectral line-scan data for the Broken Cart fire overlayed on DEM data (100 m contours). (a) Broken Cart fire imaged at 15:03 [Run 3], and (b) Broken Cart Fire imaged at 15:09 [Run 4], (c) Visual band image of the Broken Cart fire at 15:09 [Run 4]. The arrow in (a) indicates the synoptic wind direction.

Figure 8. (a) Line-scan image [Run 4] of the Blue Range fire channelling event (b) Photograph of the Blue Range fire channelling event (Photo taken by S.R. Wilkes). A fire trail, indicated in each panel, can be used to assist in matching locations in the images. Note that the image in panel (a) has been rotated to assist in this respect also.

Figure 9. Output from the terrain-filter model calibration. The thick black lines enclose the three Broken Cart fire channelling events at Log Hut Creek (bottom), Browns Creek (top left) and Cooleman Creek (top right). Thin black lines are 10-minute isochrones estimated from the available evidence, which indicate the lateral spread during the fire channelling events. The calibrated model (σ = 10.5° and δ = 33°) was applied assuming θ_w = 120°.

Figure 10. Fire channelling events, 18 January 2003. Thin black curves are 50m topographic contours, while the thick black curves enclose regions where fire channelling was observed (see Table 3). Grey grid cells indicate the parts of the landscape identified by the terrain-filter model. The model was applied assuming θ_w = 120° and parameter values of σ = 10.5° and δ = 33°.

Figure 11. Probability of wind reversal on four different slopes (when the synoptic wind direction puts them in the lee of their defining ridge) plotted against a threshold synoptic wind speed. The legend gives the general aspect and the approximate inclination of each slope. The figure was adapted from the empirical joint wind direction distributions considered in Sharples et al (2010). We note that the lower probabilities associated with the NW-facing slope are due to the generally more stable nature of easterly air masses over the Canberra region.

Figure 12. Schematic diagrams illustrating the hypothetical mechanisms suggested by the modelling results. (a) fire channelling along an incised valley, (b) fire channelling across a lee-slope.

Tables and Figures

Table 1.

RGB Assignment: R ≡ Band 11 (8.5 -13.0 µm), G ≡ Band 9 (1.55 -1.75 µm), B ≡ Band 3 (520-600 nm)					
Feature	**Pseudo-colour**	**R**	**G**	**B**	**Variants**
Active Flame	Yellow	255	255	0	Tends to be at saturation.
Decaying Flame	Bright orange	240	150	0	Intensity varies with time since ignition.
Cooling - Smouldering	Dark orange	240	70	0	Speed of cooling depends on the amount of large (slow burning) fuel.
Burnt but cool	Dark burgundy	90	20	0	Varies with terrain shading.
Unburnt forest	Dark green-brown	100	120	0	Varies with terrain shading.
Unburnt grassland	Light green	200	240	0	Varies with terrain shading and shrub density.
Shadow of dense smoke	Dark red	120	20	0	Varies with density – largely a modifier to vegetation signature.
Hot gas	Green-Blue	0	125 - 255	0 - 255	Tends to be distorted due to proximity to scanning sensor.
Hot gas over flame	White	255	255	255	

Table 1. Indicative RGB coordinate values for features in images with well balanced pixel intensity distribution. The wavelength range of Band 3 is 520-600 nm (Green), Band 9 is 1.55-1.75 µm (Mid-Infrared) and Band 11 is 8.5-13.0 µm (Thermal Infrared).

Figure 1.

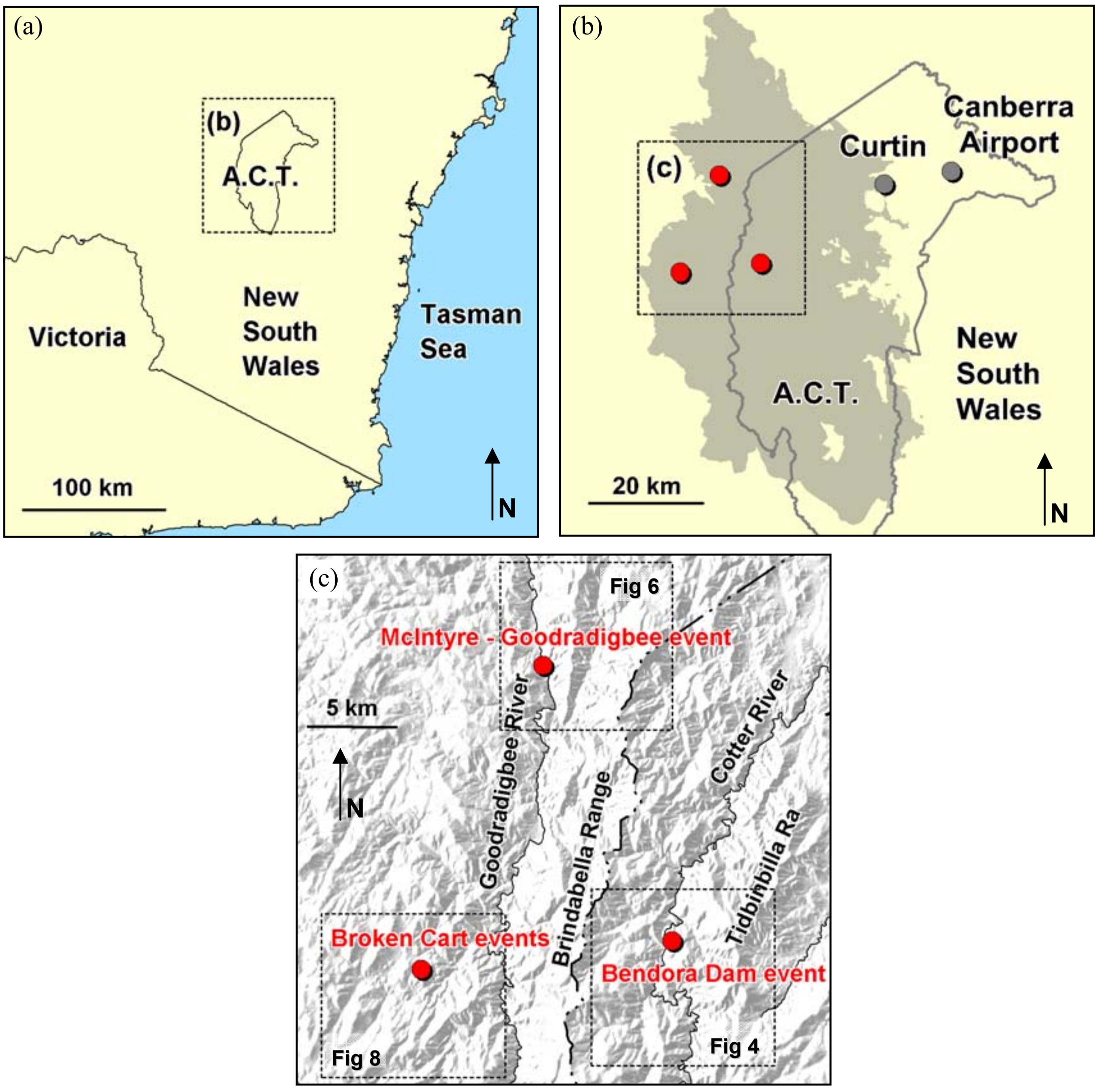

Figure 1. (a) Map of southeastern Australia showing the locations of events considered in the study, (b) Map showing the locations of the Flea Creek, Broken Cart and Bendora Dam events in relation to the main geographic features and topography of the region.

Figure 2.

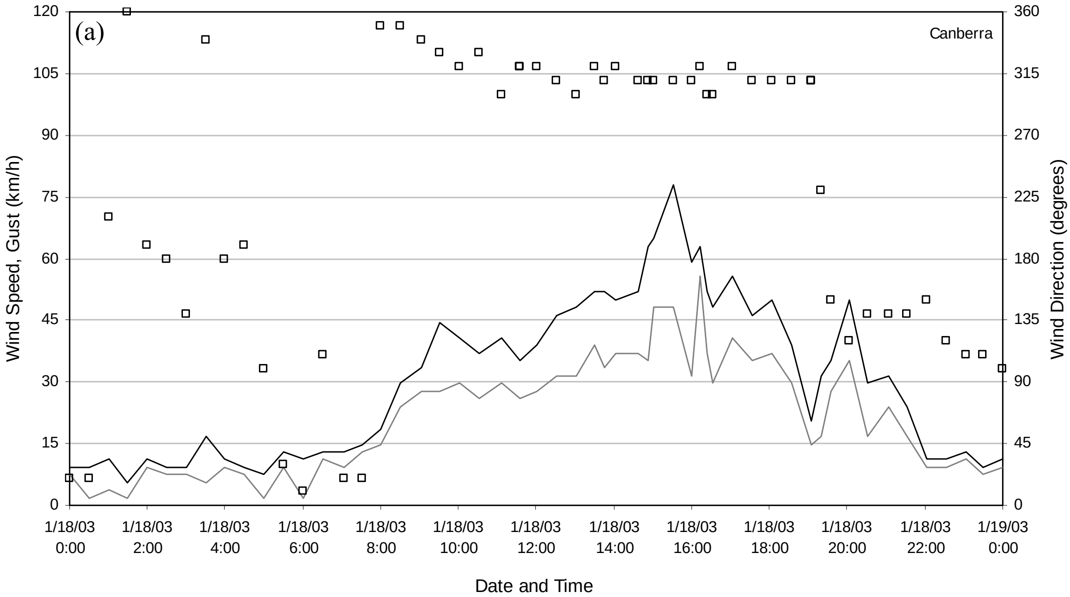

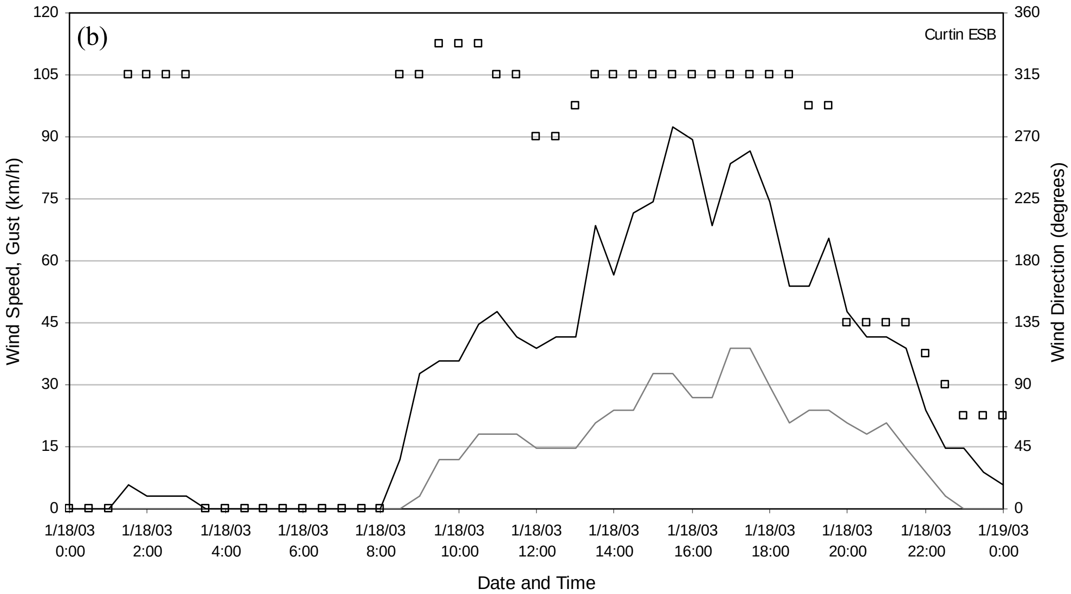

Figure 2. Wind speed (grey lines), gust (black lines) and direction (boxes) data recorded at (a) Canberra Airport and (b) Curtin Emergency Services Bureau Headquarters on 18 January 2003.

Figure 3

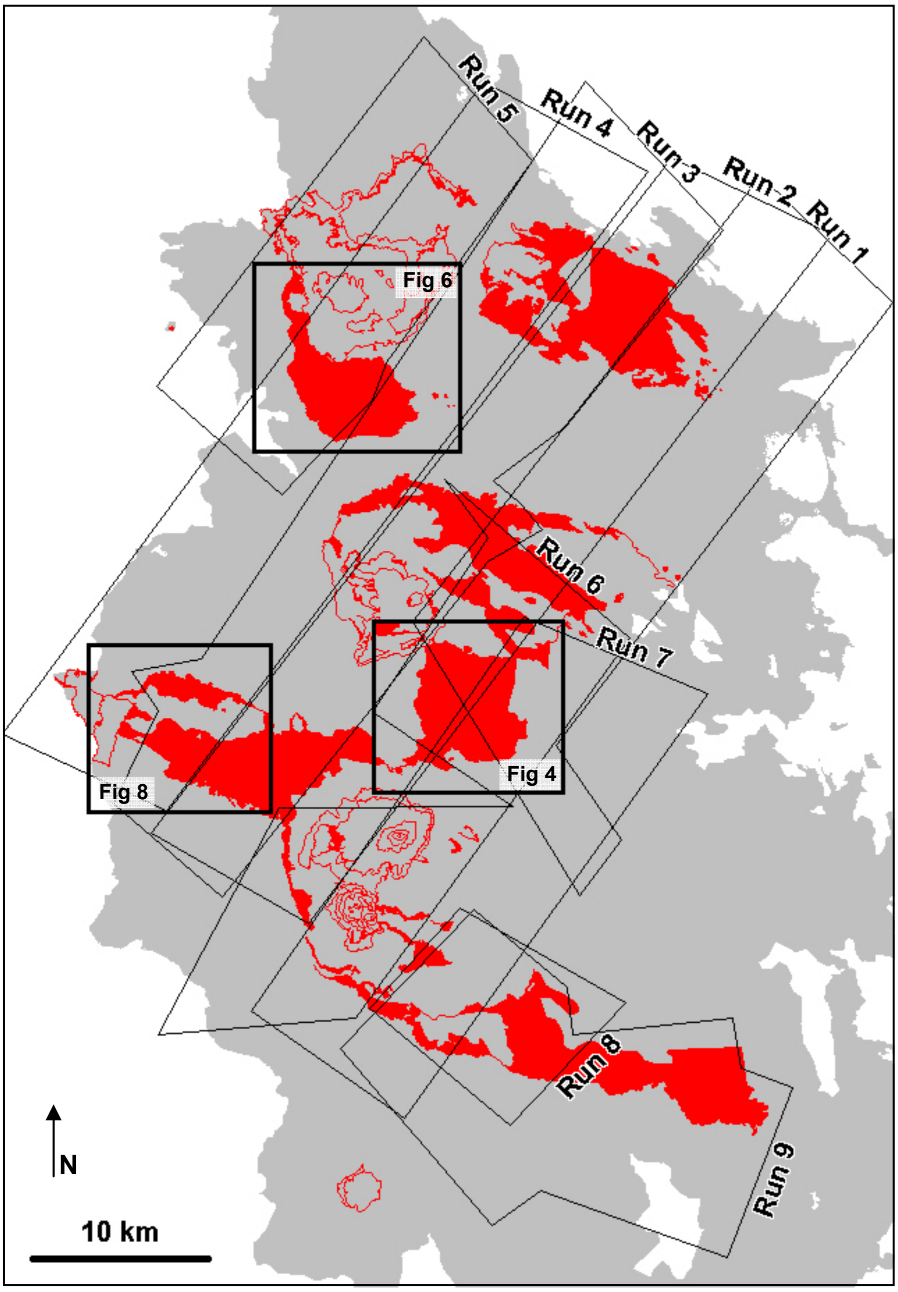

Figure 3. Multispectral line-scanning missions flown on 18 January 2003. Thin red lines indicate fire development prior to 18 January, while filled-in red regions indicate fire development captured in the line-scan imagery. The grey shading indicates the ultimate extent of the fires. The three thick black boxes indicate the extent of Figs. X, X and X.

Figure 4.

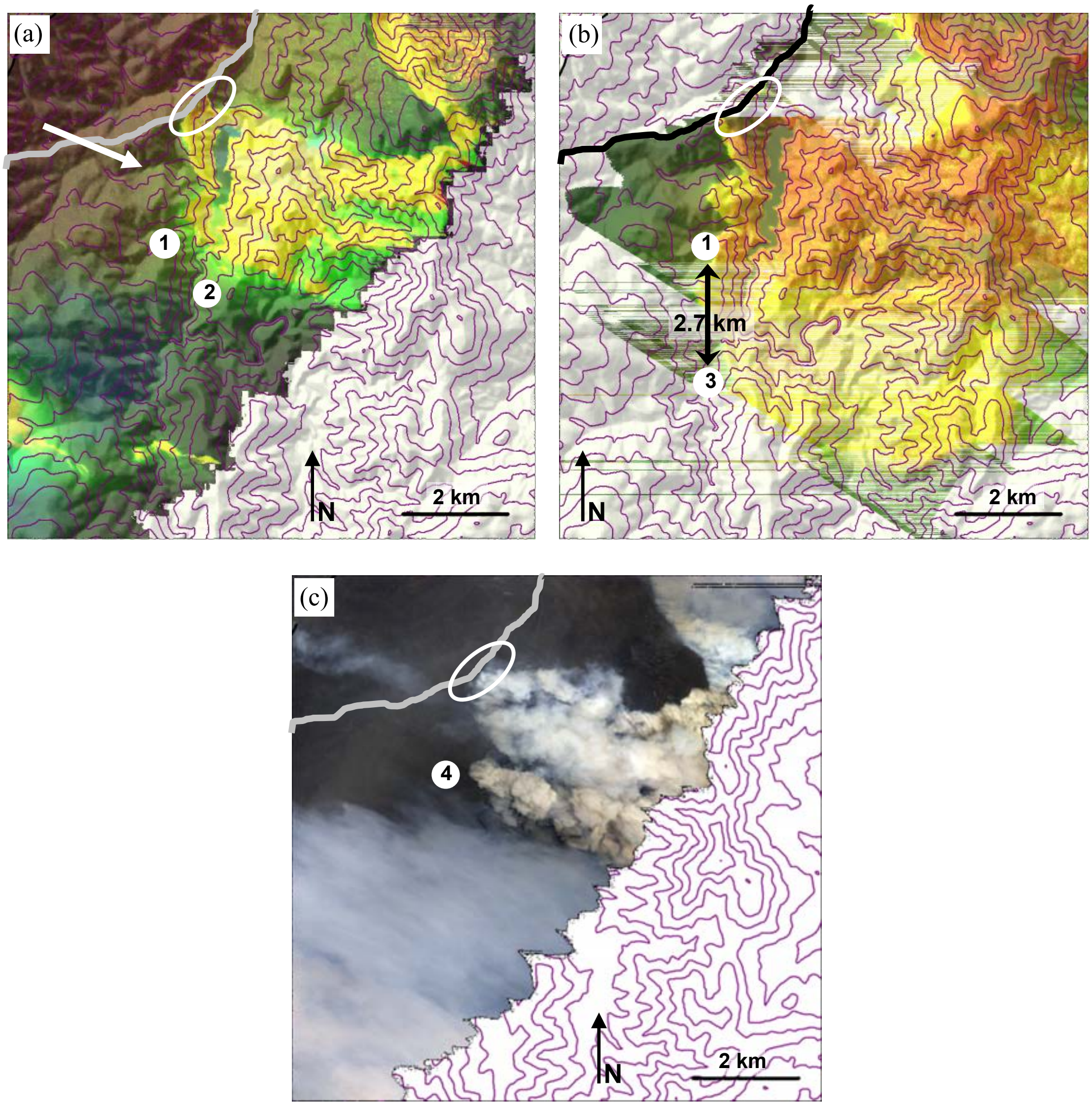

Figure 4. Multispectral line-scan data for the Bendora Dam Fire overlayed on DEM data (100 m contours). (a) Bendora Dam event imaged at 14:46 [Run 2], (b) Bendora Dam event imaged at 15:32 [Run 6], clearly moving southwards, (c) Visual band image of Bendora Dam event at 14:46 [Run 2]. The circled region in (a) is where the fire reignited. The arrow in (a) indicates the synoptic wind direction, while the grey marks the extent of the fire at 16:00, 15 January – the line was established by back burning operations. This line remained static until the spill-over occurred at approximately 14:30, 18 January. The horizontal lines evident in panel (b) are a consequence of the turbulent environment in which the aircraft carrying the line-scanning instrument was operating.

Figure 5.

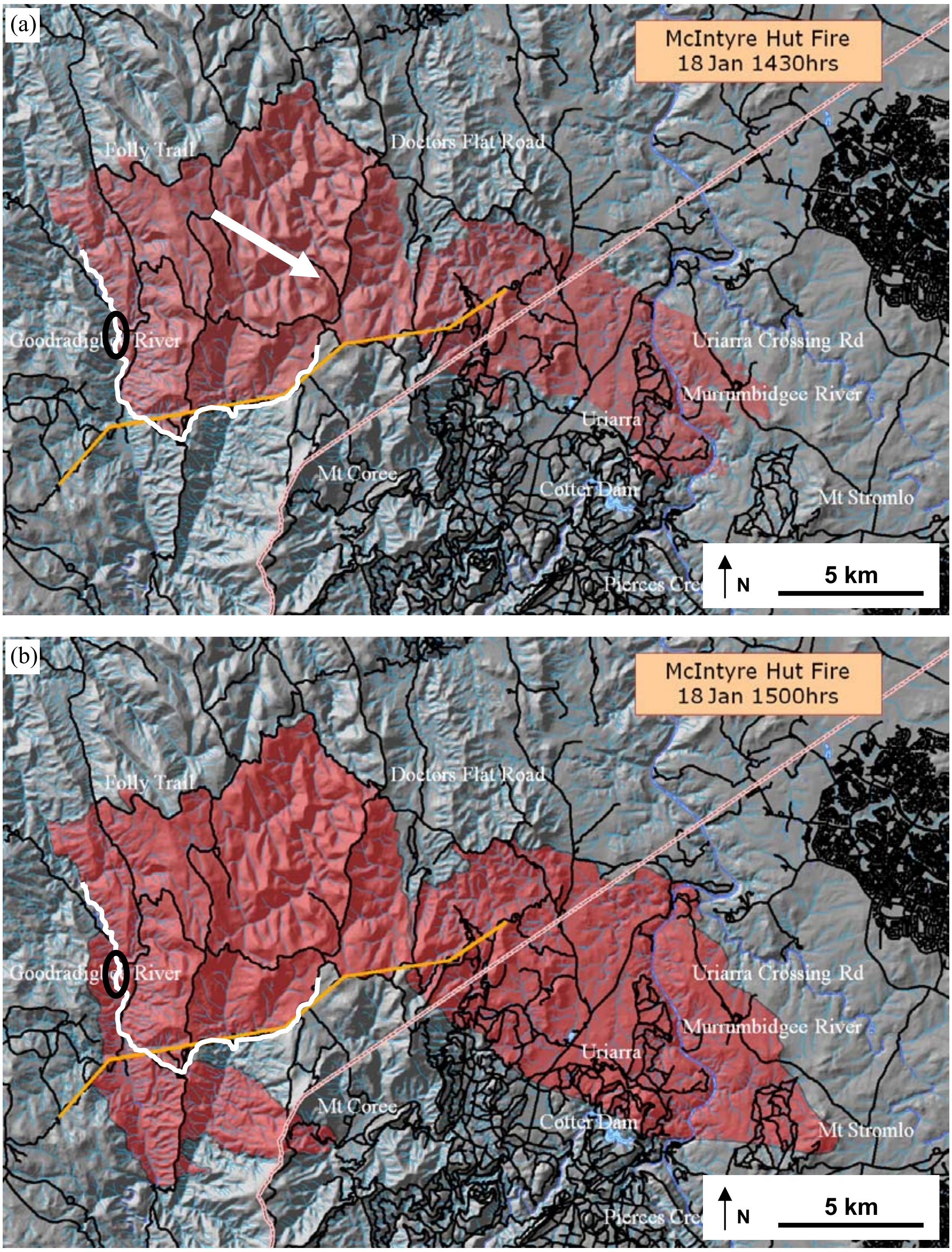

Figure 5. Evolution of the McIntyre's Hut Fire: (a) Estimated extent of the fire at 14:30, 18 January 2003, (b) Estimated extent of the fire at 15:00, 18 January 2003. The arrow in (a) indicates the synoptic wind direction, while the white line in (a) and (b) indicates the south-western extent of the fire over the period l8:30, 13 January – 14:30, 18 January 2003. The region circled in black marks the approximate position where the fire flared up. The figures were taken from slides 68 and 69 of Cheney (2003) and are reproduced with the permission of the ACT Coroner.

Figure 6

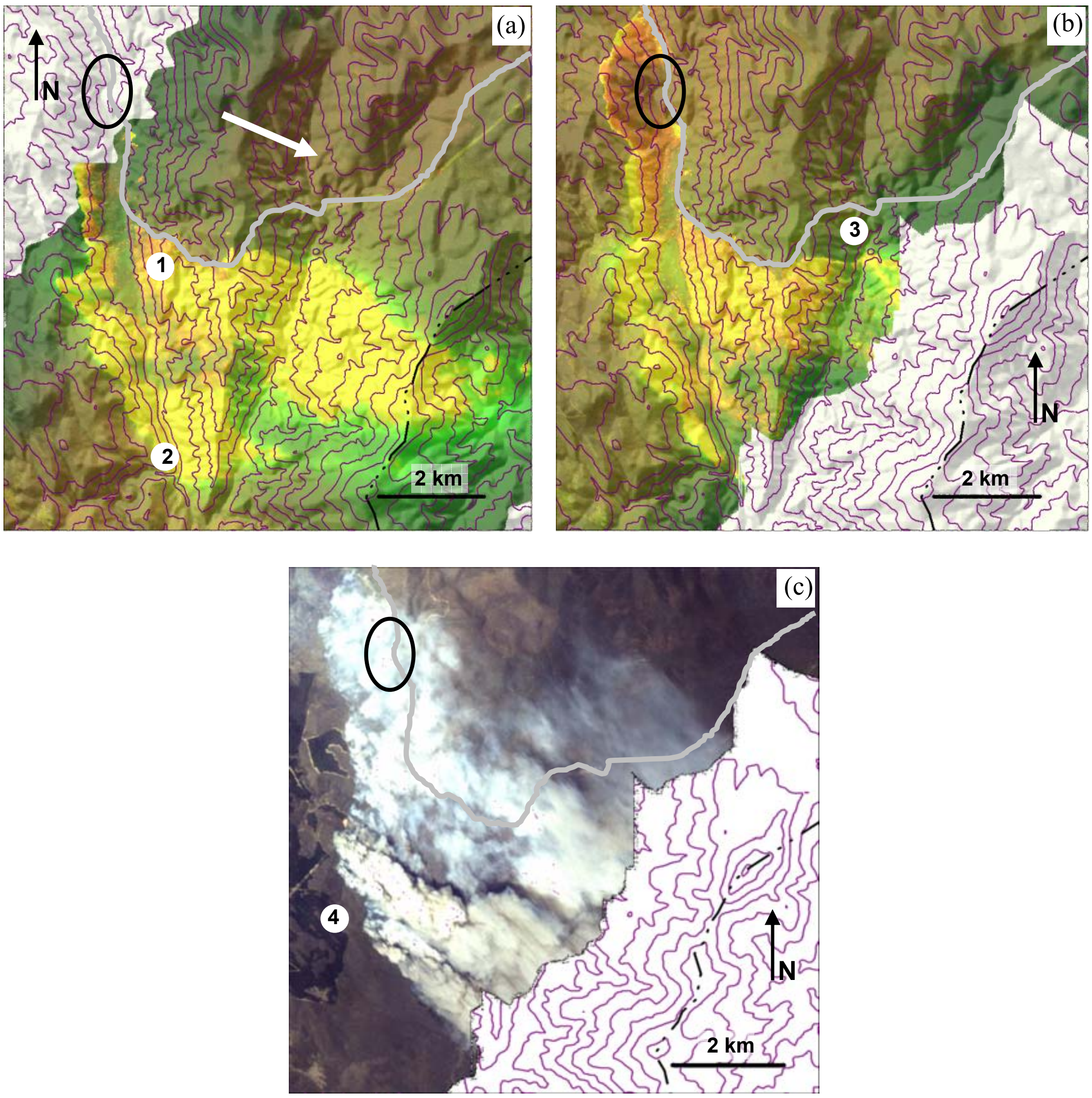

Figure 6. Multispectral line-scan data for the McIntyre's Hut Fire overlayed on DEM data (100 m contours). (a) Flea Creek – Goodradigbee River part of the McIntyre's Hut Fire imaged at 15:13 [Run 4], (b) Flea Creek – Goodradigbee River part of the McIntyre's Hut Fire imaged at 15:22 [Run 5], (c) Visual band image of the Flea Creek – Goodradigbee River part of the McIntyre's Hut Fire imaged at 15:22 [Run 5]. The arrow in (a) indicates the synoptic wind direction, while the grey line marks the south-western extent of the fire for the four day period from 18:30, 13 January to 14:30, 18 January. The region circled in black marks the approximate position where the fire flared up.

Figure 7.

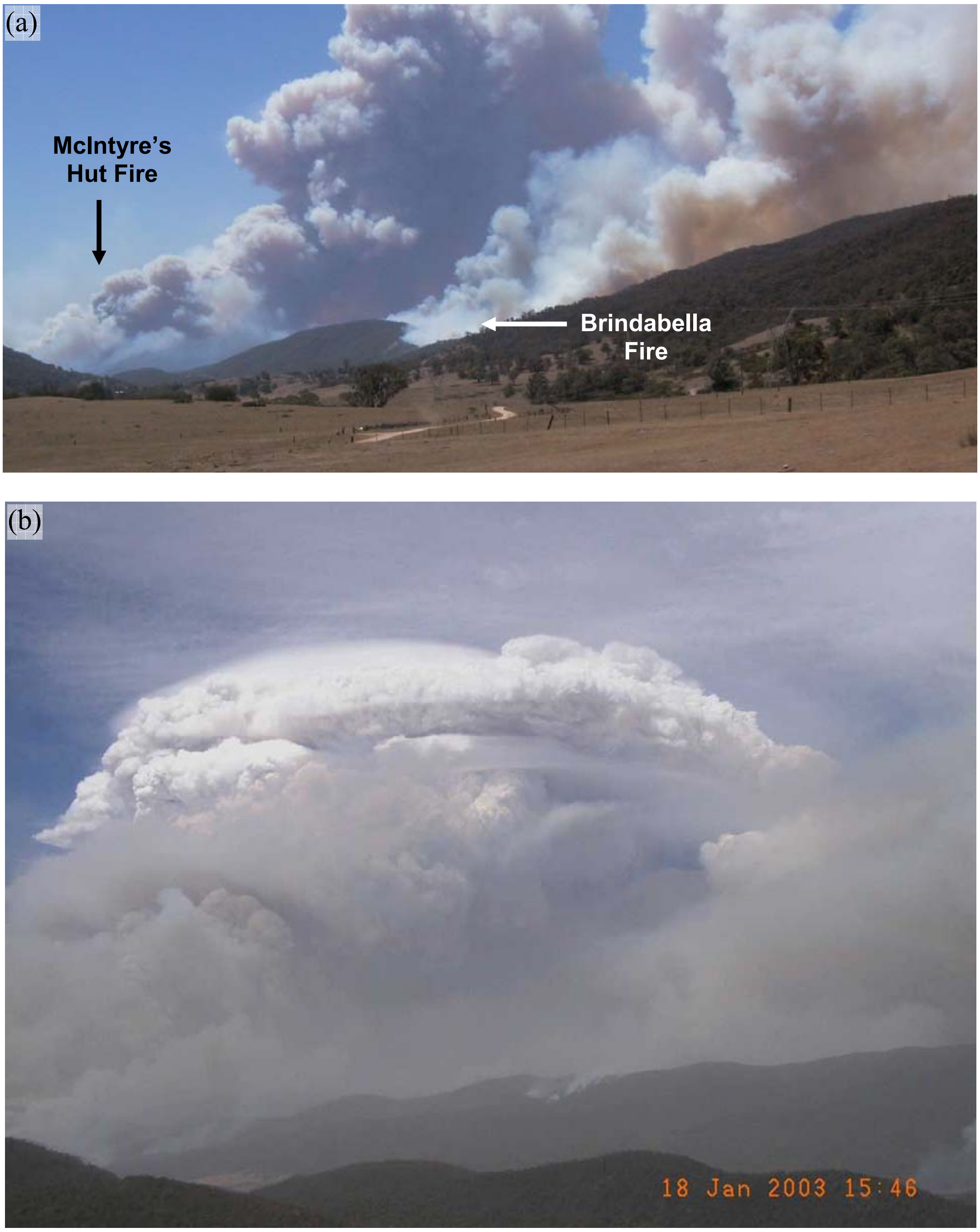

Figure 7. (a) Photograph of the fire channelling events at Flea Creek (McIntyre's Hut fire) and Brindabella Rd Lower (Photo taken by local resident), (b) Photograph of a well developed pyro-Cb over the McIntyre's Hut fire 24 minutes after the line-scan imagery in Fig. 4b was recorded (Photo taken by S.R. Wilkes)

Figure 8.

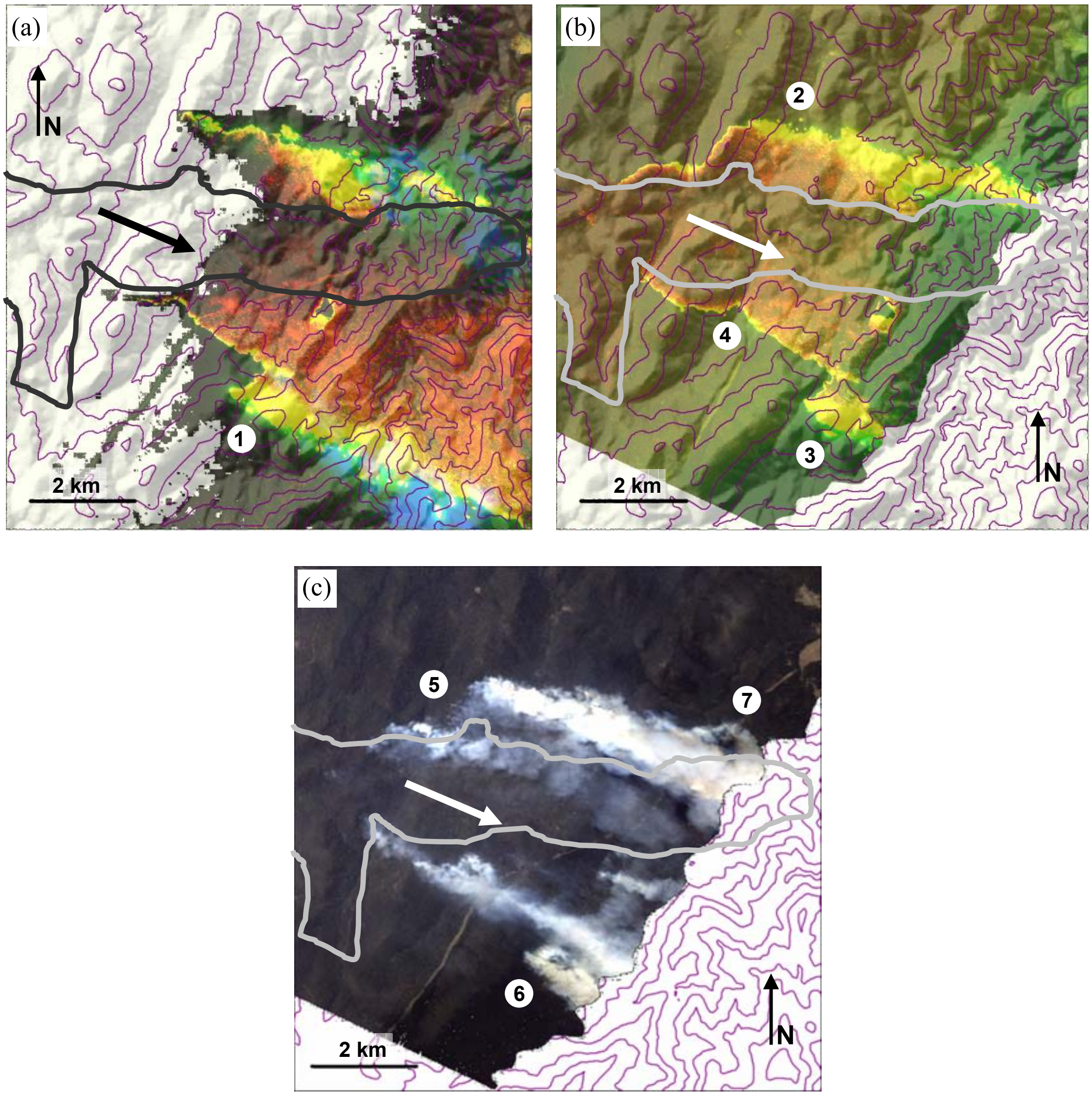

Figure 8. Multispectral line-scan data for the Broken Cart fire overlayed on DEM data (100 m contours). (a) Broken Cart fire imaged at 15:03 [Run 3], and (b) Broken Cart Fire imaged at 15:09 [Run 4], (c) Visual band image of the Broken Cart fire at 15:09 [Run 4]. The arrow in each panel indicates the synoptic wind direction, while the grey line marks the approximate location of the fire perimeter prior to 18 January.

Figure 9.

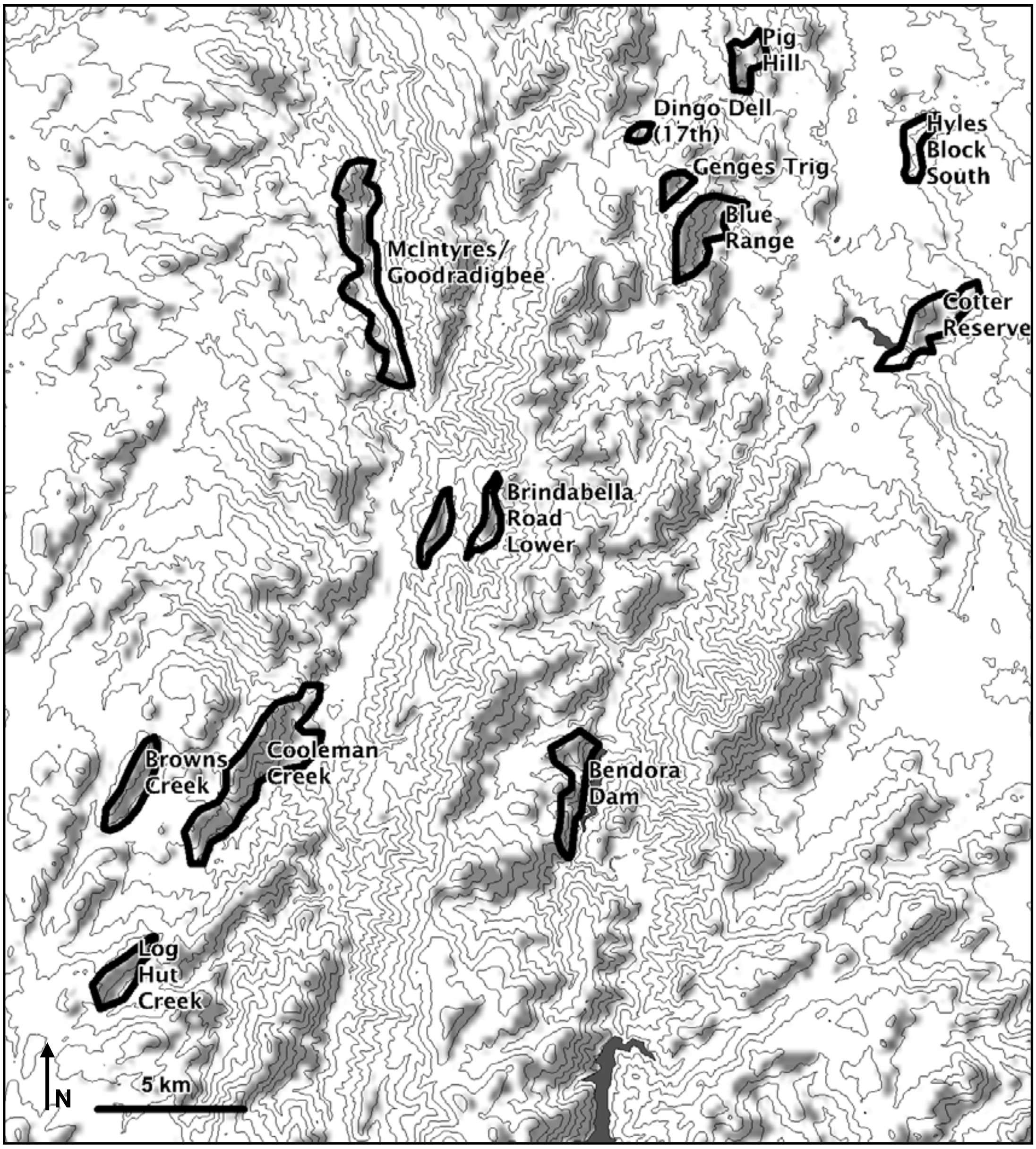

Figure 9. Fire channelling events, 18 January 2003. Thin black curves are 100m topographic contours, while the thick black curves enclose regions where fire channelling was observed. Grey shading indicates parts of the landscape identified by the terrain-filter model. The model was applied assuming θ_w = 125° and parameter values of σ = 10.5° and δ = 40°.

Figure 10.

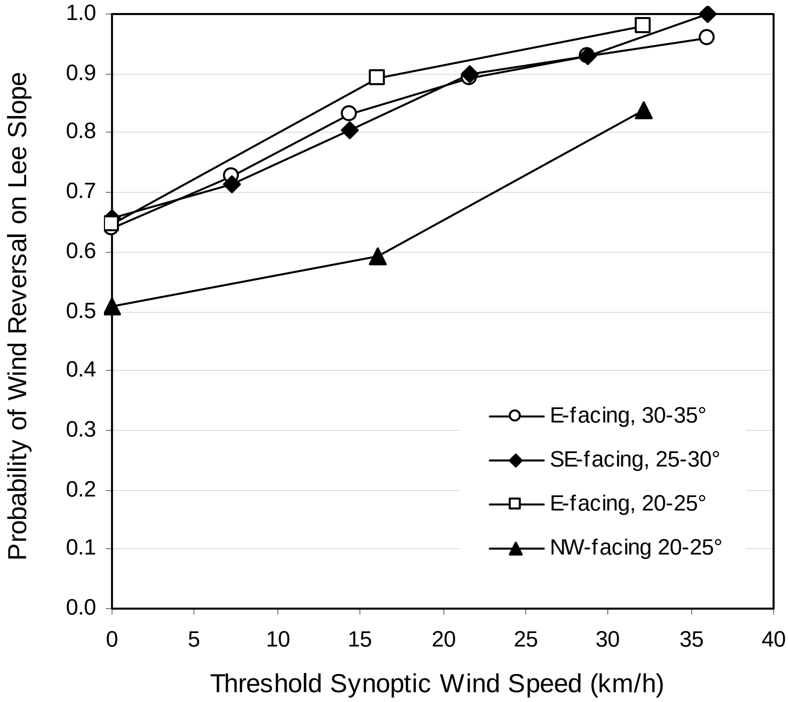

Figure 10. Probability of wind reversal on four different slopes (when the synoptic wind direction puts them in the lee of their defining ridge) in the Canberra region plotted against a threshold synoptic wind speed. The legend gives the general aspect and the approximate inclination of each slope. The figure was adapted from the empirical joint wind direction distributions considered in Sharples et al (2010). We note that the lower probabilities associated with the NW-facing slope are due to the generally more stable nature of easterly air masses over the Canberra region.

Figure 11.

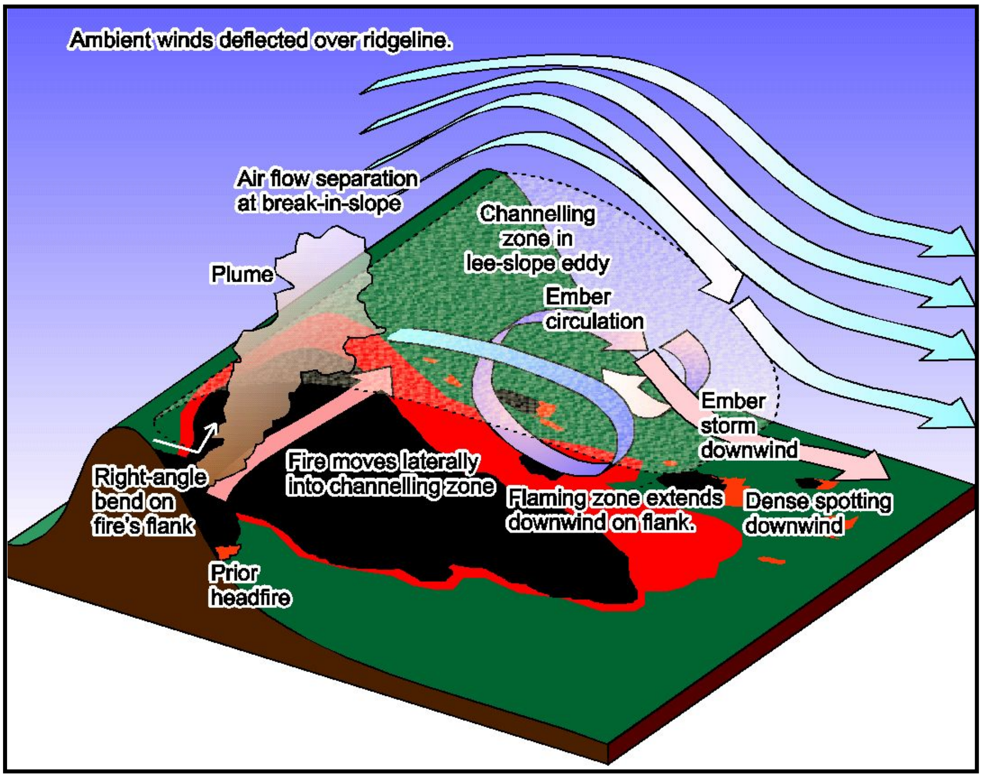

Figure 11. Schematic diagrams illustrating the hypothetical mechanism suggested by the modelling results.